Comparative study of SnO_2:Sb transparent conducting films produced by various coating and heat treatment techniques

M.A. Aegerter *, A. Reich, D. Ganz, G. Gasparro, J. Pütz, T. Krajewski

Department of Coating Technology, Institut für Neue Materialien-INM, Im Stadtwald, Gebäude 43, D-66123 Saarbrucken, Germany

Abstract

Transparent electrically conducting SnO_2:Sb coatings have been prepared by the sol–gel dip-coating process from an ethanolic solution of $SnCl_2(OAc)_2$ and $SbCl_3$ (5 mol%). The room temperature resistivity of the dip-coated films heat treated in a furnace or by laser IR irradiation is systematically greater than that obtained for films made by spray pyrolysis. Solution precursors and stabilisers and above all the deposition technique are the principal factors which influence the film morphology and hence the electrical properties. Single layers heat treated in a furnace are porous and consist of small, spherical shaped crystalline particles aggregated in a loose structure with a thin but denser top layer. A model of multilayers connected electrically in parallel allows us to determine the electrical parameters of the bulk and interface parts of the layers. Sintering by CO_2 laser irradiation increases the particle size and the packing density resulting in a resistivity that is four times less than for the conventionally furnace heat treated samples. © 1997 Elsevier Science B.V.

1. Introduction

Transparent electrically conducting coatings (TEC) on glass are used today in a wide range of optoelectronic applications [1,2]. The materials which present the most interesting properties are n-type semiconductors such as indium tin oxide (ITO), fluorine or antimony doped tin dioxide (FTO, ATO) and to a minor extent zinc oxide (ZO) doped with Al (AZO) and Ga (GZO). Practically all known coating processes have been used to deposit them [1]. Transparent ITO and SnO_2:F coatings prepared by sputtering and spray pyrolysis techniques, respectively, are available commercially with resistivities as low as 2×10^{-4} Ω cm.

The sol–gel process [3] has been successfully applied for producing indium tin oxide (ITO) coatings [4–9]. Their electrical and their optical properties are dependent on the solutions and the temperature and atmosphere used during the sintering process. The smallest resistivities have always been obtained after sintering at relatively high temperatures (600°C or higher) and the best published value of $\rho = 1.8 \times 10^{-4}$ Ω cm [7] is comparable to those typically obtained by other processes.

Few research reports have been addressed to the preparation of sol–gel antimony doped tin dioxide (ATO) coatings. Most of the sols have been prepared from Sn(IV)-alkoxides such as Sn-ethoxide [10–12], Sn-propoxide [5,13], Sn-butoxide [14–16] or more complex systems [15–18]. $SnCl_4$ [15,16,19,20], $SnCl_2$ [15,16], Sn(II)-2-ethylhexanoate [15,16,21], and Sn(II)-citrate [22] have also been used. Antimony doping usually is obtained by the addition of $SbCl_3$ [19,23,24], $Sb(OEt)_3$ [11–13,15,16] or $Sb(OBu)_3$ [5,17,21] whereas fluorine doping has not yet been achieved by the sol–gel process. The use of

* Corresponding author. Tel.: +49-681 302 5017; fax: +49-681 302 5249; e-mail: aegerter@inm.uni-sb.de.

PII S0022-3093(97)00134-8

sol stabilisers is only reported for a few solutions [13,15,16,22].

SnO_2:Sb sol–gel coatings obtained until now present a relatively high resistivity, the smallest value of $\rho = 3 \times 10^{-3}$ Ω cm [12] exceeding by more than an order of magnitude those obtained for coatings prepared by other methods (e.g., $\rho = 1 \times 10^{-5}$ Ω cm for the activated reactive evaporation of SnO_2 and SnO_2:Sb [25]).

The reasons for which highly conductive SnO_2:Sb films cannot be obtained by the sol–gel process are still unknown. The influence of the chemical composition of the sol on the resistivity of the coatings has been studied in detail by Pütz et al. [15,16]. The conductivities of the coatings are strongly dependent on the type of precursor. The use of an adequate stabiliser was found essential for the $SnCl_4$-based solution as the high chloride content of the solution leads to both volatile antimony and tin compounds which are lost during early stages of the firing process [15,26]. On the other side the stabilisers have little influence in alkoxide-based sols which have to be stabilised only against uncontrolled hydrolysis [15,27]. Chatelon et al. [11] observed a minimum in the film resistivity when the dip-coating procedure was performed in an atmosphere of ~ 35% RH. The resistivity increases when alkaline impurities are present in the coating and SiO_2 [28] or TiO_2 [13,28] buffer layers were found necessary when alkaline glass substrates are used. Another important factor is the coating microstructure which consists of small (~ 6 to 8 nm), almost spherical grains aggregated in a rather loosely packed structure after calcination at a temperature lower than 800°C [13,16,29–31]. For pure SnO_2 coatings the grain growth is suppressed and the grain size increased with film thickness [31].

This paper presents experimental results on the influence of the densification processes conditions on the electrical properties of spray pyrolytic coatings and of single and multilayer dip-coated SnO_2:Sb films sintered either conventionally in a furnace or by CO_2 laser irradiation.

2. Experimental

Single and multilayer sol–gel coatings have been obtained by dip-coating either on borosilicate glass or fused silica substrates at a withdrawal speed of 2 to 10 mm/s. The coating solution contained 5 mol% $SbCl_3$ in a 0.5 M ethanolic solution of $SnCl_2(OAc)_2$. The sintering was performed in air either in a furnace or by cw CO_2 laser irradiation which is described elsewhere [32,33]. Coatings have also been obtained by spray pyrolysis using the same solution on a borosilicate substrate at 550°C. The electrical properties have been determined by four-probe or the van der Pauw technique [34,35] with a 0.3 T magnetic field. Transmission electron microscopy (TEM) cross-sections were used to obtain information on layer morphologies. The coating thickness was measured with a surface profiler.

3. Results

Fig. 1 shows the temperature dependence of the resistivity of SnO_2:Sb single layers with a thickness of about 100 nm, dip-coated on borosilicate glass and fused silica substrates. The morphologies of SnO_2:Sb layers produced by different techniques are shown as TEM cross-sections for a 177 nm thick spray pyrolysed coating (Fig. 2), for a 70 nm thick dip-coated layer and a dip-coated multilayer system heat treated in a furnace at 550°C for 15 min Figs. 3 and 5, and for a 100 nm dip-coated layer that has been fired by CO_2 laser irradiation Fig. 8. The variation of the resistivity with the number of coatings is given in Fig. 4 for multilayer films with the same total thickness (200 nm) prepared with 2, 4, 6, 8 or 10 layers by heat treatment of each layer in a furnace at 550°C for 15 min. A plot of ρ^{-1} versus the number of deposited coatings of these data is shown in Fig. 6 where the straight line has been fitted by linear regression. Fig. 7 shows the variation of resistivity as a function of the laser power density for a 100 nm thick dip-coated SnO_2:Sb single layer on a silica substrate heat treated by CO_2 laser irradiation.

4. Discussion

4.1. Influence of the deposition technique

The room temperature resistivities, ρ, of single 90 to 105 nm thick SnO_2:Sb layers heat treated in a

Table 1
Electrical parameters of Sb doped SnO_2:Sb single layers prepared by different techniques from the same solution (0.5 M $SnCl_2(OAc)_2$, 5 mol% $SbCl_3$) (measured at 25°C)

Technique and substrate	n (10^{20} cm^{-3})	μ (cm^2/V s)	ρ (10^{-3} Ω cm)	$R_\square$ (Ω$_\square$)	Thickness (nm)
Furnace 550°C, 15 min, borosilicate	2.0 ± 0.3	1.7 ± 0.2	15 ± 0.5	1300 ± 1	110 ± 4
Furnace 700°C, 15 min, fused silica	3.3 ± 0.3	2.1 ± 0.2	8.9 ± 0.4	940 ± 1	95 ± 4
CO_2 laser, fused silica	4 ± 1.2	5 ± 1.3	3.2 ± 0.1	250 ± 1	120 ± 5
Spray pyrolysis, 4 cycles, borosilicate	4.2 ± 0.3	9.7 ± 0.7	1.5 ± 0.1	77.0 ± 0.6	177 ± 7

furnace at different temperatures for 15 min are shown in Fig. 1. For coatings deposited on fused silica substrates ρ decreases with increasing temperature to a value of 9×10^{-3} Ω cm. The increase observed with a borosilicate glass substrate at temperatures above 550°C is probably due to the onset of Na^+ diffusion from the substrate into the layer. However, the smallest resistivity is still a factor ten larger than that obtained for spray pyrolysed films using the same sol (Table 1).

The layers have different morphologies as seen from the TEM cross-sections shown in Figs. 2 and 3. The layer prepared by spray pyrolysis consists of large crystallites, densely packed in a columnar texture (cassiterite type) and presents an irregular surface. The morphology of the dip-coated film is composed of small (6 to 8 nm), almost spherical crystallites (untextured cassiterite structure) that are loosely packed. The layer is porous but its top surface (interface) is smooth and denser than the rest of the layer.

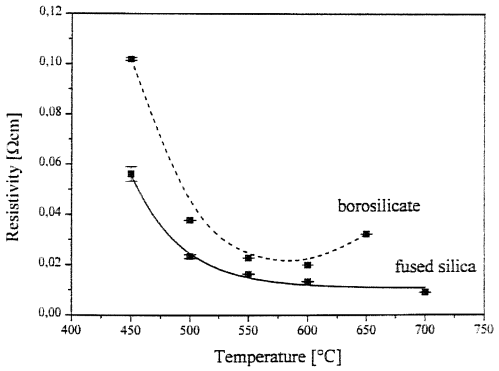

Fig. 1. Room temperature resistivity versus sintering temperature for single SnO_2:Sb layers of about 100 nm thickness dip-coated on borosilicate glass and fused silica substrates. The error bars give the standard deviation of the mean of 12 measurements. The lines are drawn as guides for the eye.

The smaller resistivity of the spray coated film is due to the presence of large and closely packed crystallites which allow a higher electron mobility. The small crystallite size and above all the porous structure observed in sol–gel dip-coated single layers lead to lower electron mobility, μ, and consequently to a larger resistivity.

The smooth surface and the small crystallite size observed in the dip-coated sol–gel layers produce less light scattering effects. Hence, the coatings have a larger optical transparency and a less hazy optical appearance than those obtained by spray pyrolysis where light scattering is larger and decreases the optical quality of the layers.

4.2. Influence of multiple coatings

The room temperature resistivities of coatings with the same final thickness (200 nm), made by

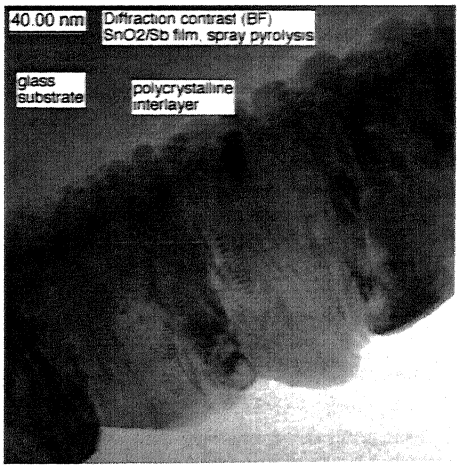

Fig. 2. TEM cross-section of a 177 nm thick spray pyrolysed SnO_2:Sb coating.

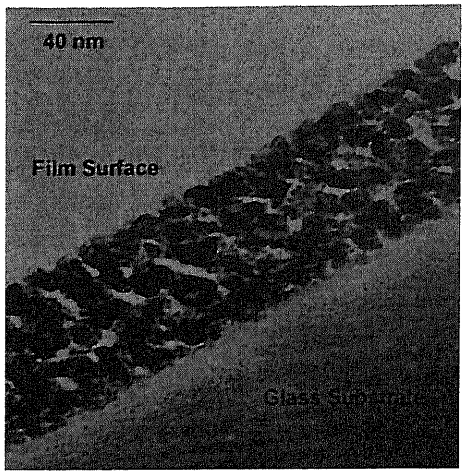

Fig. 3. TEM cross-section of a 70 nm thick dip-coated single layer SnO_2:Sb coating heat treated at 550°C during 15 min in a furnace.

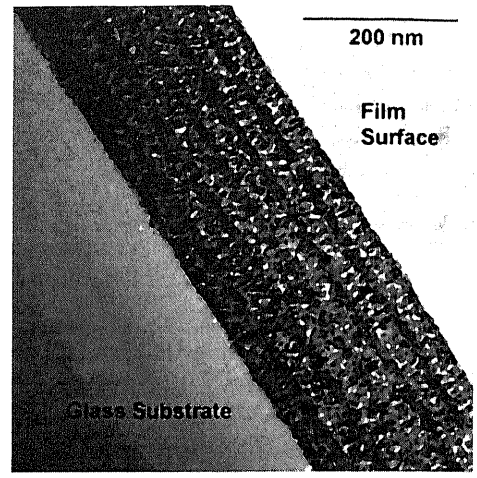

Fig. 5. TEM cross-section-micrograph of a dip-coated multilayer SnO_2:Sb coating heat treated at 550°C during 15 min in a furnace.

repeating two to 10 times the procedure of dip-coating and subsequent firing without pre-drying in air at 550°C for 15 min, decreases with the number of layers deposited (Fig. 4). This phenomenon can be understood in terms of layer morphology as shown by the TEM cross-section (Fig. 5) which reveals that each individual layer consists of a thin (< 10 nm) and relatively dense interface (external part) lying on top of a more porous material (internal part). Consequently for the same total thickness an increasing number of layers increases the fraction of denser material in the film and as mentioned above decreases the overall resistivity of the coating. Assuming therefore that the dense interfaces present a lower resistivity (ρ_e) than the internal part of each layer (ρ_i) it is easy to show that the resistivity of such a sequence of layers connected electrically in parallel is $\rho(n)^{-1} = n \cdot \rho(1)^{-1} - (n-1) \cdot \rho_i^{-1}$ where $\rho(n)$ is the measured resistivity of an n-layers coating (Fig. 6). Assuming 10 nm thick interfaces we determined from the obtained results that $\rho_i \cong 200$ Ω cm and $\rho_e \cong 1.8 \times 10^{-3}$ Ω cm.

This simple model also predicts that the product $\mu(n) \cdot N(n)$, where $\mu(n)$ and $N(n)$ are the measured

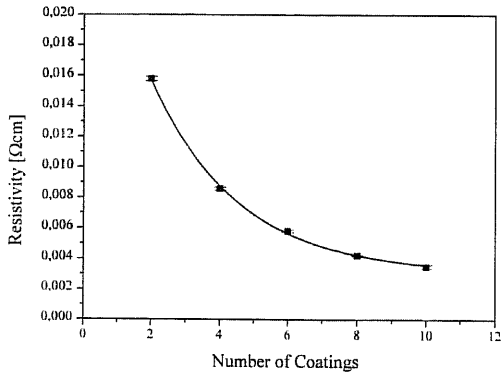

Fig. 4. Room temperature resistivity ρ versus the number of layers deposited by dip-coating (same total thickness of 200 nm). The error bars give the standard deviation of the mean of 12 measurements. The line is drawn as a guide for the eye.

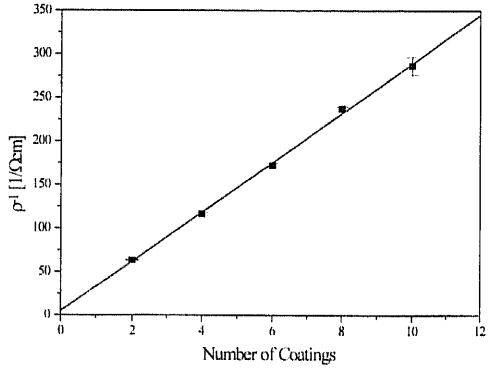

Fig. 6. Reciprocal of the measured resistivity ρ^{-1} versus the number of layers deposited by dip coating (same total thickness of 200 nm). The error bars give the standard deviation of the mean of 12 measurements. The straight line is a linear regression best fit of the data.

electron mobility and the carrier density of the n-layers coating, increases linearly with n. This allows the calculation of the mobility and carrier density of the dense layer to $\mu_e \cong 9\ cm^2/V\ s$ and $N_e \cong 4 \times 10^{20}\ cm^{-3}$, respectively. Additionally it can be assumed that the product $\mu_i \cdot N_i$ is smaller than $9 \times 10^{19}\ (V\ s\ cm)^{-1}$ for the underlying porous layer. Low resistivities in furnace sintered sol–gel coatings can therefore only be obtained if very thin layers of about 10 nm thick are sequentially deposited. A 400 nm thick coating made in this way would have a sheet resistance of about 40 $\Omega_{\square}$. As the layers will be very homogeneous with a smooth coating-air interface their optical transmission in the visible range should remain higher than that obtained for a spray pyrolysed coating of similar thickness.

4.3. Influence of the firing process

The origin of the dense interface observed in Fig. 5 is not yet known. In order to investigate if the heating rate plays a role, single layer coatings have been sintered by using a slow scan process cw CO_2 laser irradiation [32,33]. The layer thickness was found to decrease with the laser energy density and both X-ray reflectometry and Rutherford back scattering (RBS) data have confirmed that this reduction is effectively due to a densification process. The resistivity of single layers decreases with increasing laser power density to a value four times lower than

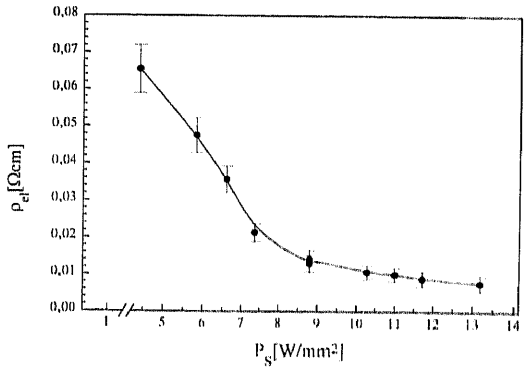

Fig. 7. Room temperature resistivity vs. the laser power density for single layer SnO_2:Sb coatings sintered by slow scan cw CO_2 laser irradiation (thickness varies with the power density). The error bars represent the standard deviation in the measured values of each sample. The line is drawn as a guide for the eye.

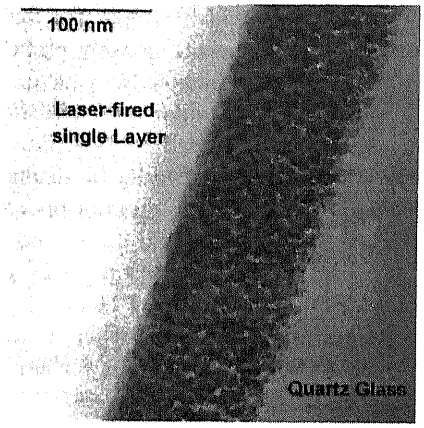

Fig. 8. TEM cross-section of a laser fired SnO_2:Sb coating ($\rho = 3.2 \times 10^{-1}\ \Omega$ cm).

that obtained for a dip-coated film of the same thickness (Fig. 7 and Table 1). TEM cross-section (Fig. 8) shows that such layers are still made of small untextured crystallites which are packed more densely. This denser structure is thought to be responsible for the lower resistivity. The resistivities obtained by laser densification are comparable to those calculated for the top interface layer observed in furnace heat treated samples. However, this technique should allow the obtention of SnO_2:Sb TEC coatings presenting sheet resistances of about 80 $\Omega_{\square}$ for a 400 nm thick coating consisting of only 3 layers.

5. Conclusion

Transparent electrically conducting sol–gel SnO_2:Sb coatings made by sol–gel dip-coating have larger resistivities than those made by spray pyrolysis. The chemical composition of the solutions plays a role while the major differences arise from the morphologies of the layers produced by the different coating technologies and heat treatment techniques. Contrary to spray pyrolysed layers which consist of large, textured, densely packed particles arranged in a columnar structure, the sol–gel layers are built of small, almost spherical, loosely packed crystalline particles with a thin dense top interface. The resistivity decreases for multilayer coatings. The overall morphology of single sol–gel layers sintered by slow

scan CO_2 laser irradiation is similar but the film is composed of larger and more densely packed particles. Their resistivity is smaller by a factor 4 when compared to coatings of similar thickness sintered in a furnace. SnO_2:Sb dip-coated sol–gel films still do not exhibit a low enough resistivity for display application. However, due to their superior optical transmission in the visible range and easier and cheaper preparation such coatings can substitute advantageously for TEC coatings (ITO, FTO, etc.) prepared by other deposition techniques when a resistivity higher than 80 $\Omega_{\square}$ is sufficient as for antistatic or heating applications.

Acknowledgements

The authors deeply thank A. Klein for the TEM preparation.

References

[1] K.L. Chopra, S. Major, D.K. Pandya, Thin Solid Films 102 (1983) 1.
[2] C.G. Granqvist, Thin Solid Films 193&194 (1990) 730.
[3] C.J. Brinker, G. Scherer, Sol–Gel Science (Academic Press, San Diego, CA, 1990).
[4] N.J. Arfsten, R. Kaufmann, H. Dislich, German patent DE 3300589 A 1 (1984).
[5] M. Mattox, Thin Solid Films 204 (1991) 25.
[6] T. Furusaki, K. Kodaira, in: High Performance Ceramic Films and Coatings, ed. P. Vincenzini (Elsevier Science, Amsterdam, 1991) p. 241.
[7] O. Yamamoto, T. Sasamoto, M. Inagaki, J. Mater. Res. 7 (1992) 2488.
[8] Y. Takahashi, H. Hayashi, Y. Ohya, Mater. Res. Soc. Symp. Proc. 271 (1992) 401.
[9] K. Nishio, T. Sei, T. Tsuchiya, J. Mater. Sci. 31 (1996) 1761.
[10] A. Maddalena, R. Del Machio, S. Diré, A. Raccanelli, J. Non-Cryst. Solids 121 (1990) 365.
[11] J.P. Chatelon, C. Terrier, E. Bernstein, R. Berjoan, J.A. Roger, Thin Solid Films 247 (1994) 162.
[12] C. Terrier, J.P. Chatelon, R. Berjoan, J.A. Roger, Thin Solid Films 263 (1995) 37.
[13] Y. Takahashi, Y. Wada, J. Electrochem. Soc. 137 (1990) 267.
[14] J.C. Giuntini, W. Granier, J.V. Zanchetta, A. Taha, J. Mater. Sci. Lett. 9 (1990) 1383.
[15] J. Pütz, diploma thesis, Universität des Saarlandes, Saarbrücken (1996).
[16] G. Gasparro, J. Pütz, D. Ganz, M.A. Aegerter, Proc. Eurosun '96, Freiburg, Germany, 1996.
[17] J.R. Gonzales-Oliver, I. Kato, J. Non-Cryst. Solids 82 (1986) 400.
[18] S.-S. Park, J.D. Mackenzie, Thin Solid Films 258 (1995) 268.
[19] D.E. Stilwell, S.-M. Park, J. Electrochem. Soc. 129 (1982) 1501.
[20] R.S. Hiratsuka, S.H. Pulcinelli, C.V. Santilli, J. Non-Cryst. Solids 121 (1990) 76.
[21] A. Tsunashima, H. Yoshimizu, K. Kodaira, S. Shimada, T. Matsushita, J. Mater. Sci. 21 (1986) 2731.
[22] P. Olivi, E.C. Pereira, E. Longo, J.A. Varella, L.O.S. Bulhoes, J. Electrochem. Soc. 140 (1993) L81.
[23] G. Gowda, D. Nguyen, Thin Solid Films 136 (1986) L39.
[24] B. Orel, U. Lavrencic-Stangar, Z. Crujak-Orel, P. Bukovec, M. Kosec, J. Non-Cryst. Solids 167 (1994) 272.
[25] H.S. Randhawa, M.D. Matthews, R.F. Bunshah, Thin Solid Films 83 (1981) 267.
[26] D.C. Bradley, E.V. Caldwell, W. Wardlaw, J. Chem. Soc. (1957) 3039.
[27] M.J. Hampden-Smith, T.A. Wark, C.J. Brinker, Coord. Chem. Rev. 112 (1992) 81.
[28] W. Lada, A. Deptula, T. Olczak, W. Torbicz, D. Pijanowska, J. Sol–Gel Sci. Tech. 2 (1994) 551.
[29] M. Kanamori, M. Takeuchi, Y. Ohya, Y. Takahashi, Chem. Lett. (1994) 2035.
[30] D.J. Yoo, J. Tamaki, N. Miura, S.J. Park, N. Yamazoe, J. Electrochem. Soc. 142 (1995) L105.
[31] D.J. Yoo, J. Tamaki, S.J. Park, N. Miura, N. Yamazoe, J. Am. Ceram. Soc. 79 (1996) 2201.
[32] D. Ganz, G. Gasparro, J. Otto, A. Reich, N.J. Arfsten, M.A. Aegerter, J. Mater. Sci. Lett., accepted.
[33] D. Ganz, A. Reich, M.A. Aegerter, these Proceedings, p. 242.
[34] L.J. Van der Pauw, Philips Res. Rep. 13 (1958) 1.
[35] A.A. Ramadan, R.D. Gould, A. Ashour, Thin Solid Films 239 (1994) 272.